Experimental and Theoretical Investigation of Effect of Spacer Arm and Support Matrix of Synthetic Affinity Chromatographic Materials for the Purification of Monoclonal Antibodies

Laura Zamolo,[†] Matteo Salvalaglio,[†] Carlo Cavallotti,*[,†] Benedict Galarza,[‡] Chris Sadler,[‡] Sharon Williams,*[,‡] Stefan Hofer,[§] Jeannie Horak,*[,§] and Wolfgang Lindner[§]

Department of Chemistry, Materials and Chemical Engineering "G. Natta", Politecnico di Milano, Via Mancinelli 7, 20131 Milano, Italy, ProMetic BioSciences Ltd., 211 Cambridge Science Park, Milton Road, Cambridge CB4 0WA, United Kingdom, Department of Analytical Chemistry and Food Chemistry, University of Vienna, Waerhringer Strasse 38, 1090 Vienna, Austria

Received: February 25, 2010; Revised Manuscript Received: May 31, 2010

The aim of this study was to elucidate the influence of each material component—the support, the spacer, and the surface chemistry—on the overall material performance of an affinity type purification media for the capture of immunoglobulin G (IgG). Material properties were investigated in terms of an experimental evaluation using affinity chromatography as well as computer modeling. The biomimetic triazine-based A2P affinity ligand was chosen as a fixed point, while spacer and support were varied. The investigated spacers were 1-2-diaminoethane (2LP), 1,3-propanedithiol (SS3), 3,6-dioxo-1,8-octanedithiol (DES), and a 1,4-substituted [1,2,3]-triazole spacer (TRZ). The support media considered were the agarose (AG) resins, PuraBead, the polyvinylether, Fractoprep, the polymethacrylate, Fractogel, and the porous silica, Fractosil. All materials were tested with pure IgG standard solution, with a mock feed solution as well as real cell culture supernatant. The interaction between IgG and A2P linked through the investigated spacers to AG was studied using molecular dynamics. The effect of a modification of the support chemical structure or of the protein−ligand binding site on the material performances was studied through target oriented simulations. Dynamic binding experiments (DBC) revealed that the performances of materials containing 2LP spacers were significantly decreased in the presence of Pluronic F68. The simulations indicated that this is probably determined by the establishment of intermolecular interactions between the 2LP charged amino group and the ether oxygen of Pluronic F68. The spacer giving the highest IgG dynamic binding capacity when Pluronic F68 was present in the feed was TRZ. The simulations showed that, among the investigated spacers, TRZ is the only one that prevents the adsorption of A2P on the support surface, thus suggesting that the mobility and lack of interaction of the ligand with the support is an important property for an affinity material. Both experiments and calculations agree that the chemistry of the support surface can have a significant impact on IgG binding, either affecting the IgG DBC, as found experimentally for materials having similar ligand densities and spacer arms but different supports, or competing with the affinity ligand when hydrophobic groups are added to the model surface, as was computationally predicted.

1. Introduction

The production and purification of monoclonal antibodies (Mabs) has been attracting considerable attention in recent years for their rising importance in diagnostic and therapeutic treatment of diseases such as immunodeficiency, Alzheimer's syndrome, and cancer.[1−4] The large scale manufacture of Mabs is an expensive process, characterized by high costs of both upstream and downstream processing.[5,6] To date the most commonly used purification process for Mab capture is affinity chromatography using protein A and protein G.[7−9] These protein-based ligands are highly selective for immunoglobulin G (IgG) showing high binding capacities of about 26−38 g/L at 10% break through for monoclonal antibodies from cell culture supernatant.[10] For pure antibody solutions of polyclonal IgG, binding capacities of up to 36−50 g/L were found.[11] The major drawbacks of protein A and protein G type adsorbents are however their elevated cost for production, making their use for Mab isolation rather expensive. In addition, protein A adsorbents have a tendency to exhibit leakage of the immobilized protein A and a low stability during sterilization and sanitation with hydroxide.[12,13] Such problems are a strong motivation for researchers to use bioengineering to create a new modified protein A that shows increased stability and loading efficiency[13] as well as to develop new biomimetic or peptide-mimetic affinity materials, which might make cost-effective alternatives to protein A.[14−23]

In affinity chromatography it is the design of the ligand headgroup that is investigated most with respect to the capture and purification of a target protein. However, the design of a new affinity material should also consider the chemical and physical properties of all its constituents, that is the base support matrix, the ligand headgroup, and the spacer-arm by which they are connected. Nonetheless, in affinity material development, constraints have to be reduced. Therefore the main focus is being set on the optimization of support properties and the actual

* Corresponding authors. (C.C.) Tel: +39-02-23993176. Fax: +39 02 23993176. E-mail: carlo.cavallotti@polimi.it. (J.H.) Tel: +43 1 4277 52373. Fax: +43 1 42779523. E-mail: Jeannie.Horak@univie.ac.at. (S.W.) Tel: +44 (0) 1223 433844. Fax: +44 1223 420270. E-mail: SWilliams@PrometicBioSciences.com.

[†] Politecnico di Milano.

[‡] ProMetic BioSciences Ltd.

[§] University of Vienna.

10.1021/jp1017168
Published on Web 06/30/2010

design of new ligand head groups for protein purification, mostly neglecting entirely the possible influence spacer chemistry or the surface chemistry of the support may have on the overall material performance, although their effect on the protein binding process is already known.[7] In a recent study, it was shown that ligands bound to a support with spacer arms of certain length and chemical composition can in actual fact interact with the support itself.[24] Such interactions are influenced by the physical and chemical properties of the spacer and can lead to a conformational change of the system in which the ligand, instead of being uniformly solvated by water, can be adsorbed on the support surface.[25]

The spacer contribution to the protein binding process has been the subject of several research works. Mateo and co-workers have compared different activations of agarose (AG)-type supports, finding that short spacer arms can fix the relative positions of the groups involved in the immobilization and thus increase the rigidity of the bound protein, which allowed the use of certain proteins as ligands in high performance liquid chromatography.[26] Fuentes and co-workers proposed a different interpretation of the role of the spacer-chain. They compared the efficacy of different AG matrices in the separation of a mixture of polyclonal anti-horseradish peroxidase (HRP) using HRP as a ligand. Several protocols of immobilization of HRP were compared with the performance of HRP immobilized onto AG through a long, flexible, and hydrophilic spacer arm (dextran). It was thus found that while glyoxyl−AG, monoaminoethyl-*N*-aminoethyl−AG (MANA−AG), glutaraldehyde−AG, and the commercial BrCN−AG were able to adsorb only up to 60−70% of a mixture of polyclonal anti-HRP antibodies,[27,28] HRP immobilized on dextran−AG was able to adsorb 100% of the polyclonal anti-HRP. On this basis Fuentes et al. concluded that the absence of steric hindrances plays a critical role in favoring the complete recognition of all classes of polyclonal antibodies and that a long, hydrophilic, and neutral spacer can prevent the undesirable interaction both with the target protein and the macromolecular ligand.[29]

In this context, the main goal of the here presented study is to investigate how the choice of a particular support and spacer can influence the ligands binding efficiency. Such information may be of importance for further studies in the field of material development for affinity-based capturing of Mabs. In order to investigate the possibility to actually predict material performance in advance, our study implies and compares both experimental as well as theoretical results.

At the experimental level, several new biomimetic affinity materials were prepared, which possessed the same ligand headgroup, namely the synthetic biomimetic affinity ligand A2P, also known as MAbsorbent, but differ in the composition of the base support and the connecting spacer arm (Figure 1).

Four different spacers were investigated. The first and also the shortest spacer arm was the benchmark, the simple diaminoethyl-spacer (2LP), followed by 1,3-propanedithiol (SS3), 3,6-dioxo-1,8-octanedithiol (DES), and a 1,4-substituted [1,2,3]-triazole spacer (TRZ), formed through a copper(I) mediated Huigen 1,3 dipolare azide−alkyne cycloaddition reaction (Figure 1).[30−32] These ligand−spacer combinations were coupled to four different support matrices, the cross-linked AG resins, PuraBead, from ProMetic BioSciences Ltd. (AG), the two tentacle-grafted polymeric beads, the polyacrylamide Fractoprep (FP) and polymethacrylate Fractogel (FG) from Merck KGaA, and Fractosil (FS), a porous form of silica, also from Merck KGaA. These new affinity-based materials were then tested for their ability to capture IgG from a variety of mock feed solutions as well as real cell culture supernatant.

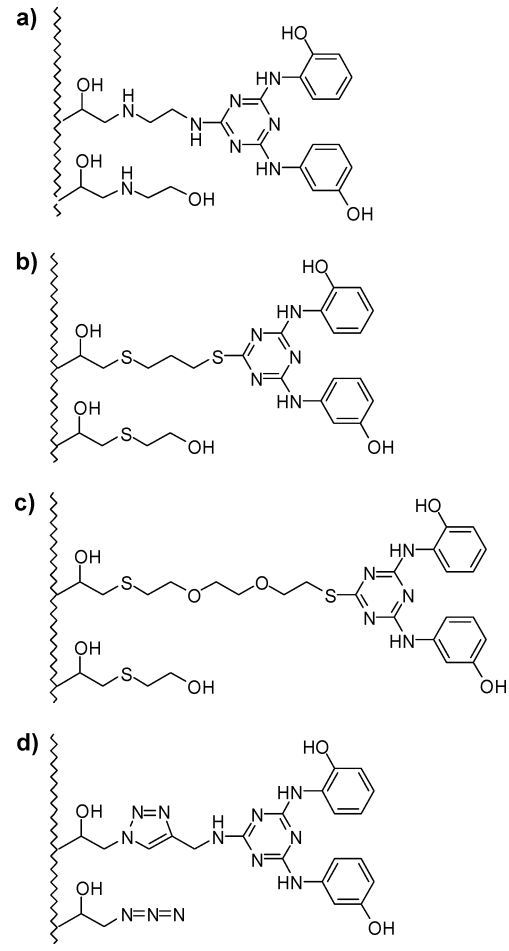

Figure 1. Chemical structures of A2P-type ligands with four different spacer arms and the end-capping strategy of the corresponding adsorbents (except of d): (a) A2P-2LP, (b) A2P-SS3, (c) A2P-DES, and (d) A2P-TRZ.

On the theoretical level, molecular dynamic (MD) and density functional theory (DFT) simulations were employed to determine the binding structure and energy of IgG with the spacer supported ligands, bound to an AG support. AG was chosen as a suitable support, since enough information is available from literature to build a reliable molecular model and it is a good model for at least one of the experimental supports, PuraBead.[33,34]

2. Experimental Section

Affinity Materials. The protocols for the synthesis of all investigated affinity ligands and their corresponding materials as well as details concerning support properties and protein quantification are described in the Supporting Information. A summary of epoxy, A2P and 2-mercaptoethanol densities of the investigated materials are listed in Table 1.

Protein Standards. Horse skeletal myoglobin (MYO), human serum albumin (HSA), and Pluronic F68 were obtained from Sigma (Poole, Dorset, U.K.). Bovine gamma globulin (BGG; 2 mg/mL) was from Pierce (Surrey, U.K.). Human polyclonal immunoglobulin G (IgG1), Sandoglobulin, was obtained from Sandoz (Hampshire, U.K.). *N*-Antiserum to human IgG and N protein standard PY reagent for nephelometric quantification of IgG were supplied by Siemens Healthcare (Surrey, U.K.). Cell culture supernatant containing human monoclonal antibody, h-IgG1 from CHO-cell expression system was obtained from

TABLE 1: List of Investigated A2P-Type Materials and Their Epoxy, Azido, and A2P-Densities As Well As the Density of the Immobilized End-Capping Reagent and the Number of Residual Azido Groups

adsorbents	epoxy density[a] [μmol/g (dry)]	azido density [μmol/g (dry)]	A2P density [μmol/g (dry)]	end-capping[b] [μmol/g (dry)]	residual azido groups [μmol/g (dry)]
AG-2LP-A2P	200		497	yes	
AG-SS3-A2P	200		231	0	
AG-TRZ-A2P	200	350	225	no	125
FG-2LP-A2P	1000		100/350	yes	
FG-SS3-A2P	1000		371	73	
FG-DES-A2P	1000		325	175	
FG-TRZ-A2P	1000	1126	335	no	790
FP-2LP-A2P	250		40/75/248	yes	
FP-SS3-A2P	250		330	237	
FP-DES-A2P	250		351	156	
FS-2LP-A2P	40		40	yes	

[a] Epoxy-densities for Fractogel (FG), Fractoprep (FP), and Fractosil (FS) are as stated by the manufacturer Merck; AG was calculated from μmol/g moist, suction dried gel (wet) using the corresponding correlation factors in Table S1 in the Supporting Information. [b] SS3-A2P and DES-A2P materials were end-capped with 2-mercaptoethanol and the end-capping efficiency determined via elemental analysis. 2LP-A2P materials were end-capped with 2-ethanolamine, but the efficiency was not determined. TRZ-A2P type materials are not azido-end-capped and the residual azido groups were determined through subtraction of the A2P-density from the originally determined azido group density on the support.

ExcellGene (Monthey, Valais Switzerland). The IgG titer of the feed was between 60 and 150 mg/L with a conductivity of 10−15 mS/cm and a pH between 6.5 and 7.5.

Three different antibody containing feed solutions were prepared and tested. The first feed solution (F1) is a mock feed of well-defined chemical composition that was designed to mimic a "real" Mab supernatant. It contains 1 g/L polyclonal IgG, 1 g/L horse skeletal myoglobin, and 5 g/L human serum albumin in PBS with pH 7.4. Alternatively 1 g/L of the antifoaming agent Pluronic F68 was added to F1. The second feed solution (F2) is a real CHO cell culture supernatant with human monoclonal IgG1. The third feed solution (F3) contains only 1 g/L of pure polyclonal IgG in PBS, pH 7.4. All feed solutions were filtered prior to use. Buffer solutions as well as cell culture feed solutions were filtered with reusable bottle top filters with 0.45 μm nitrocellulose membranes from Fisher Scientific (Loughborough, U.K.).

The total protein concentration of the chromatography samples was determined using the Bradford Coomassie protein assay kit from Pierce, (Surrey, UK). The IgG concentration of F1 and F3 were determined using nephelometry and the IgG concentration of the cell culture supernatant F2 was determined via protein A HPLC (further details are available in the Supporting Information).

Note that all chromatographic experiments were performed in a temperature controlled environment (19−22 °C) and all buffer solutions were used at room temperature. The contribution of mass transfer effects can therefore be safely neglected, especially considering that the comparison between experiments and calculations were mostly of qualitative nature.

Computer Modeling. The procedure for the MD simulations used in this work is based on the experience developed in the study of similar systems and described in detail in our previous publications and in part in the Supporting Information.[24,35] Briefly, the molecular model of the chromatographic system here comprises four parts: the antibody, the affinity ligand, the spacer, and the support. These latter three components are covalently bound and form the stationary phase and can all interact with the protein through polar and apolar interactions.

The antibody was modeled as the full Fc domain of a human IgG. Its initial coordinates were obtained from the Protein Data Bank (PDB) entry 1HZH,[2] which reports the full structure of the antibody including the two Fab domains. However, the latter were not considered in the MD simulations to reduce the size of the system. This approximation is justified by the fact that the ligand was designed to specifically interact with the Fc binding site of immunoglobulin G, which is that part of the molecule most directly involved in the adsorption process.

As mentioned, the ligand benchmark in this study is the synthetic affinity ligand A2P, while four different spacers (2LP, DES, SS3, and TRZ) were considered in the calculations.

AG, which is a good model for the PuraBead support matrix, was adopted as model of the support material. The basic structure of AG is well-defined: it consists of long fibres of alternated D-galactose and 3,6-anhydro-L-galactose units organized in double helixes, as can be noted from the crystallographic data (PDB entry 1AGA).[36] The AG crystal structure was used to build three molecular models of AG, which were successively used in the calculations. The first is the one reported in Figure S2a and was developed and adopted in our previous studies of the system.[24] To evaluate the effect that the density of hydrophobic groups on the support surface may have on the binding process, a second model was introduced. The AG surface was partially modified by substituting some of the D-galactose residues with 6-*O*-methyl-galactose residues, thus making it more hydrophobic with respect to AG. Only residues oriented toward the protein were substituted in order not to reduce the stability of the support by altering the structure of its helixes (Figure S2b). The third model of AG, sketched in Figure 2, consists of three sets of parallel double helixes and is thus three times larger than the model of Figure S2. It was used to test whether the calculations are converged with respect to the AG molecular model size.

The conformational evolution of the IgG-ligand-spacer-support system was investigated using molecular dynamics simulations. The force field adopted for the AG support was Glycam 04,[37−40] developed to study the interaction of carbohydrates with proteins, which was modified to include 3,6-anhydro-L-galactose and 6-*O*-methyl-D-galactose residues.[24] Spacers, ligands, and the protein were modeled with the Parm 94 force field,[41] supplied in the Amber suite.[42,43]

The input structures of the ligand-IgG complex were determined via docking, using AutoDock 3.0;[44] subsequently the complex was bound to the support and solvated using explicit TIP3P water molecules adding a solvent shell of 20 Å. The simulations were performed using periodic boundary conditions,

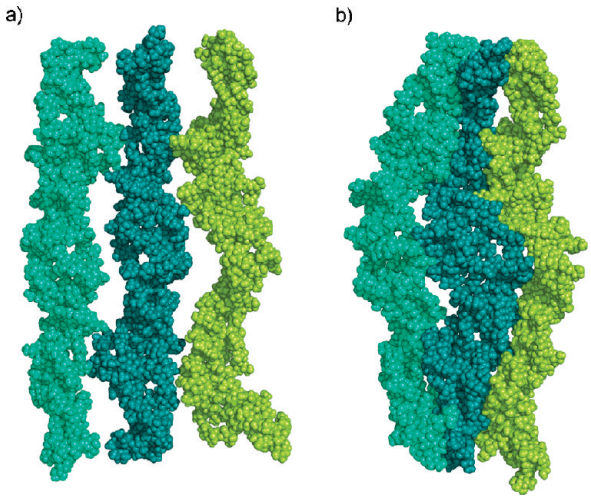

Figure 2. Structure of the molecular model consisting of three sets of intertwined double helixes at the beginning of the simulations (a) and after relaxing the system for 10 ns in water (b).

according to which the system is divided in unit cells of equal size, calculating long-range electrostatic interactions using the particle mesh Ewald method.[43]

The computational protocol adopted for the MD simulations is described in detail in our previous papers[24,35] and in the Supporting Information.

The energetic analysis of the simulations was performed calculating the difference of the interactions developed by the ligand with its surrounding environment in its "bound" (i.e., the ligand in complex with the protein) and its "free" state (i.e., the ligand not bound to its receptor). Whereas in the here-examined system the surrounding environment of the bound ligand includes the solvent, antibody, and support matrix, in the free state, it consists of support and water molecules. Thus, two different MD simulations were performed for each system: the first for the support−spacer−ligand−Fc complex (15 ns) and the second for the supported ligand alone (support−spacer−ligand). In the latter case, the simulation protocol was analogous to the one used for the complex but a shorter time span (3 ns) was considered, as this was sufficient to stabilize the system. Interaction energies were determined with the Anal. program of the Amber 8 computational suite; their medium values for the bound state were averaged on a time span of 1 ns, whereas for the free state they were averaged on all the 3 ns of the simulation.

Finally, in order to investigate what determines the significant effect that Pluronic acid has on IgG adsorption, in particular when the spacer arm changes, some additional simulations were performed using simplified molecular models of Pluronic acid and ligand. Structures were determined with the integral equation formalism polarized continuum model (IEFPCM) at the B3LYP/6-31 g(d,p) level, while energies were calculated at the B3LYP/aug-cc-pVDZ level.

MD and ab initio simulations were performed using the Amber 8 computational suite[42] and Gaussian 03,[45] respectively; all structures reported in this work were produced using Molden 4.4,[46] VMD 1.8.2,[47] and Pymol.[48]

3. Results and Discussion

The synthetic biomimetic affinity ligand investigated in this study is a disubstituted aminophenol derivative of trichlorotriazine, named A2P. It was discovered by ProMetic BioSciences Ltd. (PBL) through a Chemical Combinatorial Library for compounds active in the binding of polyclonal IgG. In combination with PBL's own proprietary base matrix PuraBead, an AG-based support, A2P is also known as MAbsorbent A2P. A2P is a well characterized affinity ligand,[22,49,50] making it a suitable candidate for our elaborate biochromatographic and computer simulation studies. It was designed for human and humanized antibodies and mimics the dipeptide binding site of Phe 132 and Tyr 133 in the hydrophobic core structure of protein A,[19] which plays an important role in the formation of a binary complex between A2P and the Fc-domain of IgG. A2P possesses an affinity (dissociation constant) for human and humanized IgG of approximately 1×10^{-4} M and provides binding capacities of 15−25 g/L for polyclonal IgG from mammalian plasma with purities of >85 and 95% respectively.[22] In validation studies using monoclonal and polyclonal IgG sources, no A2P-ligand leakage has been detected after 300 process cycles and IgG product integrity was always maintained.

In this study, the influence of support chemistry and spacer chemistry on the overall performance of a number of different new affinity materials with A2P as the main ligand motive will be discussed. They all carry the same A2P ligand headgroup but possess different spacer arms. The benchmark has a simple amino linkage (2LP) with the formula $CH_2-CHOH-CH_2-NH-(CH_2)_2-NH-$ (Figure 1a). To test the effect of spacer composition and flexibility, two thiophilic spacers differing in their chemical composition as well as length were investigated, the SS3 spacer, $CH_2-CHOH-CH_2-S-(CH_2)_3-S-$ (Figure 1b), and the DES spacer, $CH_2-CHOH-CH_2-S-(CH_2)_2-O-(CH_2)_2-O-(CH_2)_2-S-$ (Figure 1c). The fourth spacer arm contains a 1,4-substituted [1,2,3]-triazole ring, $CH_2-CHOH-CH_2-(C_2HN_3)-CH_2-NH-$, and will be referred to as TRZ (Figure 1d).

In the following sections, we will first discuss the outcome of the experimental affinity-chromatographic measurements, followed by a summary of material performance evaluation obtained by molecular dynamics simulations. In the final stage, we will then try to correlate the experimentally obtained results with the predictions obtained by computer simulation experiments.

Experimental Results. ***Affinity-Chromatography.*** Dynamic binding capacities (10%-DBC; BC) and elution recoveries (EC) for IgG on A2P bound by three different spacer arms to three different support matrixes were determined for the three different feed solutions: F1, F2, and F3. The performance of each combination of ligand, spacer arm, and support material was investigated chromatographically using the mock feed F1, which contains polyclonal IgG, myoglobin, and human serum albumin. Since Pluronic F68 is known to affect the separation process performance of certain affinity ligands due to an interaction with the ligand, additional measurements with 1 g/L of Pluronic F68 added to F1 were performed. In order to determine a possible cross-sensitivity of the investigated materials to proteins other than IgG, the concentration of HSA in the elution fractions was determined by nephelometry. The concentration of myoglobin, although also present in the feed F1, was not determined. Nonetheless, one has to consider that any additional binding of proteins other than IgG or any other compound present in the application feed will eventually reduce the overall binding capacity of the material for the target protein, IgG.

The results for the mock feed solution F1 and A2P-type materials in comparison to rmp protein A Sepharose FF are summarized in Table S2. It is clearly shown that, even for this simple mock feed solution (F1), all investigated A2P-type materials differ strongly in their performance. Binding as well as elution capacities vary depending not only on the ligand

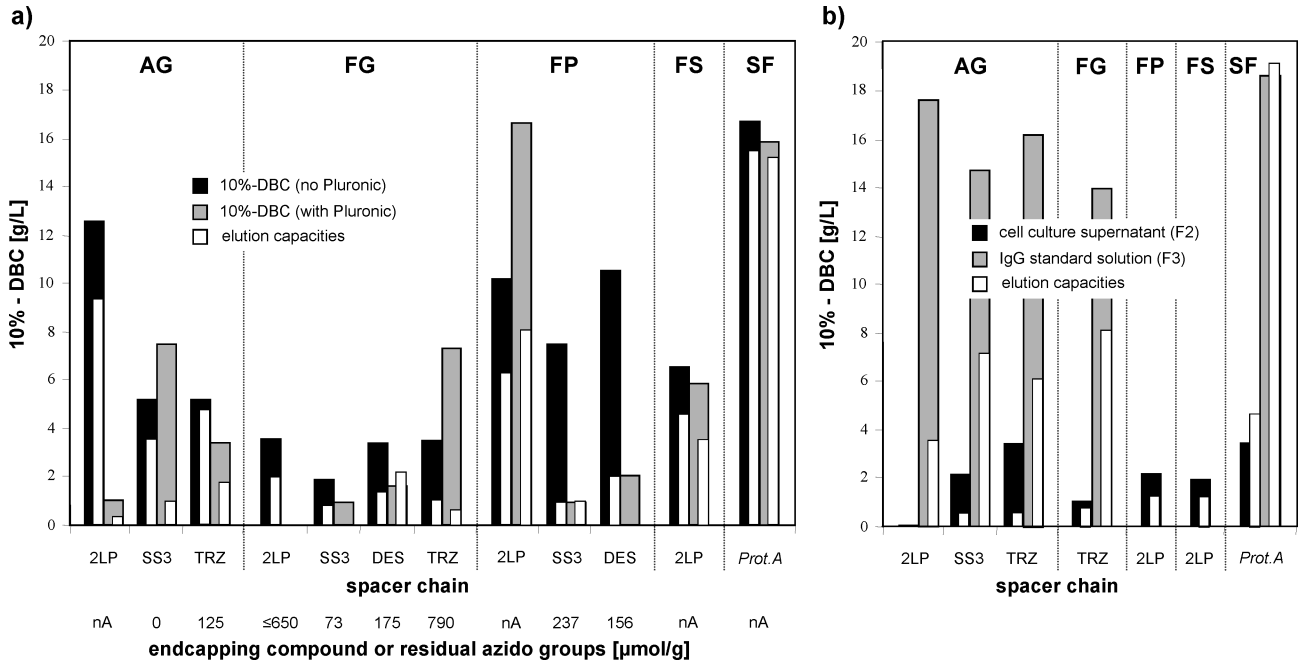

Figure 3. Material performance evaluation of A2P-type purification media investigated with (a) mock feed solution (F1) containing 1 g/L polyclonal human IgG, 1 g/L myoglobin, and 5 g/L human serum albumin with optional addition of Pluronic F68 and (b) cell culture supernatant (F2) containing 60−150 mg/L human monoclonal IgG1 plus 1 g/L sodium azide and approximately 1 g/L Pluronic F68 with a pH ranging from 6.5 to 7.5 (batch dependent) and a standard solution of polyclonal IgG in PBS buffer with pH 7.4 (F3). Support media are abbreviated as AG for AG, FG for Fractogel, FP for Fractoprep, FS for Fractosil, and SF for the rmp-protein A Sepharose FF.

density of A2P, where DBC values decrease with declining A2P-densities, but also strongly on the choice of spacer and support matrix. Surprisingly, the elution capacities are mostly lower than the corresponding binding capacities but are in some cases practically the same as it is the case for AG-TRZ-A2P using F1 without Pluronic acid, and FP3-2LP-A2P and FG-DES-A2P using F1 with Pluronic acid. Also the sensitivity of the materials toward the presence of Pluronic F68 in the test solution is differing with the change in spacer and support chemistry. Note that some materials such as FP1-2LP-A2P actually perform better in the presence of Pluronic F68. A2P-type materials with the least sensitivity toward Pluronic F68 addition are FP1-2LP-A2P with a binding capacity of 16.6 g/L, AG-SS3-A2P with 7.45 g/L, and FP3−2LP-A2P with 4.9 g/L, with only the latter providing practically same binding and elution recoveries for IgG.

Generally speaking, AG-2LP-A2P possesses the highest BC and EC values, with 12.6 and 9.4 g/L for F1 without Pluronic F68, whereas FP1-2LP-A2P performs best in the absence (BC 10.2 g/L and EC 6.4 g/L) as well as in the presence of Pluronic F68 (BC 16.6 g/L and EC 8.1 g/L).

The thiophilic A2P ligand SS3 shows a very low affinity for IgG in the presence of Pluronic F68. However in the absence of Pluronic F68, a change of support, from Fractogel to Fractoprep, provided an almost 4-fold increase in the DBC for A2P-SS3 from 1.9 g/L to 7.5 g/L. The same tendency was observed for A2P-DES and A2P-2LP, where a change of support from Fractogel to Fractoprep provided a 3-fold increase in DBC from 3.4 to 10.5 g/L and from 3.6 to 10.2 g/L, respectively.

The performance of the different A2P-type materials for the capture of IgG from feed solution F1, from a cell culture solution F2 and a standard solution of polyclonal IgG, is compared graphically in Figure 3. This plot shows clearly that material performance can not be deduced by the performance of the ligand headgroup per se but that a more or less strong fine-tuning of material performance can be achieved by introducing another spacer-arm or another support. The Fractogel sector in Figure 3a shows that, on Fractogel-type supports, the binding capacity does not vary strongly in the absence of Pluronic F68.

However, as soon as Pluronic acid is present, binding capacities for IgG become highly spacer dependent and increase in the order of spacers used: 2LP, SS3, DES, and TRZ, with no binding for the 2LP spacer, which is surprising, since the corresponding Fractoprep material FP1-2LP-A2P performs best in the presence of Pluronic F68. For AG-based supports, the introduction of the spacer arms SS3 and TRZ reduces IgG binding in the absence of Pluronic F68, but on the contrary, increases IgG binding in the presence of Pluronic F68 for AG-SS3-A2P. Here the SS3-spacer performs best, followed by the TRZ-spacer. This result for AG suggests that the addition of a thiophilic spacer arm reduces the negative impact of Pluronic F68 on the AG adsorbent and the A2P ligand. The strongest Pluronic-dependency in terms of reduced BC values in the presence of Pluronic F68 was observed for AG-2LP-A2P, FG-2LP-A2P as well as FP-SS3-A2P and FP-DES-A2P, whereas FS-2LP-A2P was least influenced.

The best performing support-spacer combinations in terms of binding capacity for IgG and Pluronic F68 sensitivity are AG-2LP, FP1-2LP, FP1-DES, AG-SS3, AG-TRZ, FG-TRZ, and FS-2LP, which were selected for further testing with real cell supernatant (F2) as well as standard IgG solution without Pluronic F68 (F3) to determine their maximum achievable binding performance for IgG without competitive protein adsorption. The results for F2 and F3 are shown in Table S3.

Figure 3b (Table S3) demonstrates clearly the biggest difference in performance. While F3 is a typical standard protein solution of polyclonal IgG in PBS (pH 7.5) without any additives, F2 resembles a real cell culture solution of a CHO-cell expression system and, as expected, the mock feed F1 in Figure 3a (Table S2) provides BC and EC values that lie in all cases between those obtained for the feed solutions F2 and F3. Highest binding capacities for IgG using the feed F3 were

obtained for the following support-spacer combinations in declining order AG-2LP-A2P > AG-TRZ-A2P > AG-SS3-A2P > FG-TRZ-A2P, though BC values only vary slightly between 14 g/L and 17.7 g/L.

On the other hand, for the cell culture solution, the binding capacities for IgG were all rather low between 1.1 g/L and 3.5 g/L. The latter was obtained for AG-TRZ, followed by AG-SS3, FP1-2LP, FS-2LP, and FG-TRZ. The significant reduction of binding capacity of IgG from 10.2 to 2.1 g/L for FP1-2LP-A2P may be explainable by the fact that this support-spacer combination binds the most feed impurities from the cell culture feed. However the least difference in binding capacity for F1 as well as for F3, with and without Pluronic F68, was observed for affinity material AG-TRZ-A2P.

Generally speaking, the results in Figure 3b (Table S3) indicate that when using a short and charged spacer arm, such as 2LP, A2P on AG-based support does not bind IgG from the cell culture supernatant. However, when a spacer arm differing significantly in length and chemical composition is introduced, either DES or TRZ, the binding capacity increases significantly. The AG-TRZ-A2P adsorbent has a similar IgG binding performance as observed for the commercially available adsorbent Rmp protein A Sepharose FF. It is worth noting that the DBC values for all of the adsorbents investigated are rather low at below 4 g/L h-IgG1, which is most likely induced by the low IgG titer of below 100 mg/L in the cell culture solution plus the more or less strong binding of feed impurities, which definitely reduces the binding capacity of the materials for IgG. This effect is most pronounced for FP1−2LP-A2P, where BC was reduced from 10.2 g/L for F1 (no Pluronic acid) to 2.1 g/L IgG for F2 (with Pluronic acid) at a BC for the feed impurities of 3.5 g/L.

Note that all investigated materials with a 2LP-spacer were end-capped by reacting the remaining epoxy-groups with ethanolamine and all materials with SS3 and DES spacers were modified with 2-mercaptoethanol. In a separate study we have shown that a deactivation of residual, still reactive epoxy or azido groups on the support surface as well as the choice of end-capping reagent to deactivate them after ligand immobilization can have a tremendous impact on the overall material performance.[51] In actual fact the introduction of additional amino-groups by using ethanolamine may lead to mixed-mode type affinity materials, where the underlying support chemistry functions as a weak anion exchanger binding feed impurities and thereby reduces the BC of the material for IgG. In case of the affinity materials with a TRZ-spacer, the here-investigated materials are all nonazido end-capped, meaning that residual azido groups are present on the material surface, which are prone to capture IgG but provide low recoveries of the latter.[51]

Additionally it should be noted that different batches of cell culture supernatant were used to test the various affinity-materials, since they were prepared and tested over a period of 2−3 years. The variations in binding and elution capacities of these investigated materials can be explained through the variation in the feed impurity composition from the various production batches of the CHO cell expression system (Figure 4a, lane 1 and Figure 4b, lane 1). Taking all of this into account, one should consider that most material manufacturers frequently state the protein binding performance of their materials only for standard protein solutions, which as we have seen will most likely not correlate with the actual material performance for real sample solutions.

Another way to characterize materials is to simply distribute the proteins by their molecular weight on slab gels. The SDS-PAGE gel in Figure 4b indicates that the presence of the TRZ spacer does improve the performance of the benchmark AG-2LP-A2P as there is significant capture and purification of IgG from the F2 feed solution. This confirms that the addition of a spacer arm increases the Pluronic F68 tolerance of the A2P ligand, as AG-2LP-A2P does not bind IgG from cell culture solution that contains Pluronic F68.

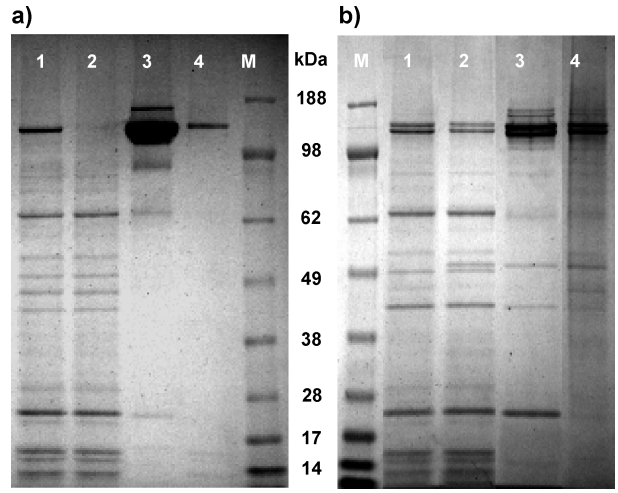

Figure 4. Nonreduced SDS-PAGE slab gels of affinity chromatographic fractions of (a) rmp-protein A Sephapose FF and (b) AG-TRZ-A2P tested with cell culture supernatant (F2), showing the feed loading (lane 1), feed flow-through (lane 2), IgG elution (lane 3), and the cleaning-in-place fraction (lane 4). Lane M shows the molecular weight marker.

In addition to improving the binding capacity of AG-2LP-A2P with the addition of spacer chemistries, it is also important to consider the effect of the spacer arm on the purity of the eluted IgG. Figure 4a shows the SDS-PAGE gel for the commercial benchmark adsorbent rmp protein A Sepharose FF. If the purity of the elution fractions in lane 3 from Figure 4, panels a and b, are compared, a pronounced feed impurity band appears at ~25 kDa for the AG-TRZ-A2P, which is less distinct for rmp-protein A Sepharose FF. This band may be excess light chain, which is already present in the feed solution, but may just as well be an unidentified feed impurity. Overall, it can be stated that Protein A binds more of the high molecular weight (MW) impurities compared to AG-TRZ-A2P, which binds more of the low MW impurities. It is noteworthy that the elution conditions for AG-TRZ-A2P have not been optimized for this cell culture feed. Furthermore the ligand immobilization concept via "click reaction" was at this point of our study not yet fully optimized. Nonetheless, the experimental results show clearly that in terms of both binding capacity and purity the incorporation of the TRZ spacer instead of the benchmark 2LP has produced an affinity adsorbent with much improved IgG capture performance, although its elution performance still needs to be optimized.

Influence of Pluronic F68 on Material Performance. In order to investigate why and how Pluronic F68 is influencing the IgG binding performance of the A2P type materials, AG-2LP-A2P was tested with mock feed F3 under three different conditions, namely without addition of Pluronic F68 (A), with 1 g/L Pluronic F68 (B), and without Pluronic F68 in the feed, but with a pretreatment of the adsorbent with 1 g/L Pluronic F68 in PBS, pH 7.4 (C). Besides that, these experiments were performed in the same manner as previously described for the testing of A2P-type support materials. However, the new additional test conditions A, B, and C should verify which of

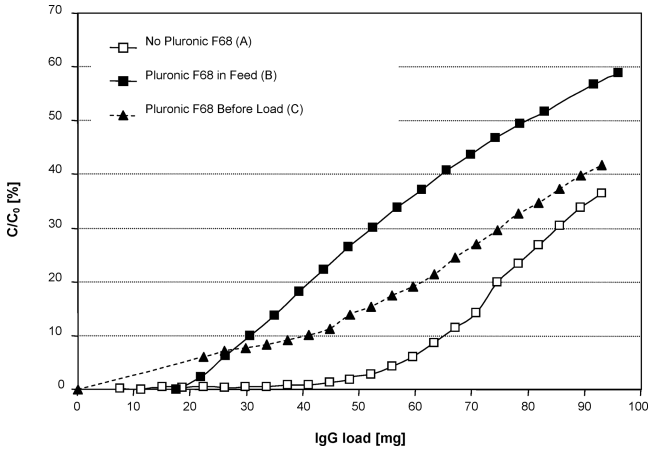

Figure 5. Break-through curve of IgG on AG-2LP-A2P tested under different conditions: (A) without addition of Pluronic F68 in the application feed, (B) with addition of 1 g/L Pluronic F68, and (C) with a material that was pre-equilibrated with PBS containing 1 g/L Pluronic F68 before addition of an application feed only containing 1 g/L IgG.

the three following hypotheses apply for AG-based A2P-type materials: first, if Pluronic F68 may interact with the IgG molecule and hinder thereby the binding to the surface bound A2P-ligand; second, if Pluronic F68 may interact with the A2P-ligand on the adsorbent surface; or third, if Pluronic F68 can actually form a complex with the AG-based matrix of the adsorbent and provide some kind of sterical hindrance preventing the IgG molecules binding to the A2P-ligand.

The breakthrough curves in Figure 5 show that for condition A a binding capacity, at 5%-DBC of 13 mg/mL adsorbent was obtained, which is more than 50% higher than for either of the two other conditions, where a 5%-DBC of 6 and 5 mg/mL were observed for conditions B and C, respectively. When Pluronic F-68 is loaded onto the material before the IgG containing feed was applied (condition C), a very early, almost immediate but shallow breakthrough of IgG was observed. It may be proposed that the binding of Pluronic F68 to AG is rather weak in nature and that due to the lack of Pluronic F68 in the application feed, some of the surface-attached Pluronic F68 molecules are being gradually washed off the surface, reducing thereby the concentration of Pluronic F68 on the material surface and increasing at the same time the binding capacity of the material for IgG. In case of condition (B), where both IgG as well as Pluronic F68 are present in the feed, the material binds first IgG and second Pluronic F68. It can be assumed that as more and more Pluronic F68 molecules attach to the surface, less IgG can bind to the A2P ligand.

The fact that Pluronic F68 affects the column both when loaded with IgG and when loaded prior to IgG clearly demonstrates that, rather than binding to the IgG molecule, Pluronic F68 is interacting with the adsorbent. Furthermore the results for A2P-2LP type ligands bound to different type of supports in Figure 3 show clearly that Pluronic-sensitivity of material performance is highly dependent on the chemistry of the support. It was observed that AG is being strongly influenced by the presence of Pluronic F68, followed by the polyacrylate-based Fractogel, the polyacrylamide-based Fractoprep and the silica-based Fractosil, of which the latter provide the most consistent results for IgG capture and elution in the presence as well as absence of Pluronic F68.

In additional experiments (data not shown), it was verified that Pluronic F68 does not desorb or replace IgG once it is securely bound to A2P. Furthermore it was found that an increase in spacer-length as well as an introduction of a specific surface-modification, through the change of chemical properties or by introduction of a physical barrier to prevent the attachment of Pluronic F68 to the support surface, can make A2P-type materials less sensitive to the presence of Pluronic F68 in the application feed.

Molecular Dynamics Simulations. ***Determination of the Protein−Ligand Binding Structures: Docking.*** The theoretical determination of the binding structure of a ligand with a large protein such as IgG is a complicated task. The problem is however slightly simplified if the favored binding sites of the protein of interest are already known. In the case of IgG, it is well-known that the Fc domain has a specific part of the surface that is usually directly involved in the formation of bonds with other proteins; this part is located at the hinge region between CH2 and CH3 domains and known as the "consensus binding site" (CBS). For these reasons the CBS has been the subject of many studies in the literature. Delano et al.[25] compared this site with several patches of the IgG surface similar in size, according to different criteria including hydrophobicity and accessible surface area, and observed that it presents a prevalent non polar nature, a high tendency to form H bonds and an elevated solvent accessibility. These features alone, however, cannot explain its predisposition for binding, since they are common to other patches and in particular to a larger region of the Fc domain comprising the consensus site. What discriminates the binding site is its high flexibility, distinctive of hinge regions, which provides the CBS with a significant conformational mobility and the possibility to adapt easily to different ligands.

The structure of the complex formed by IgG and A2P was determined through docking simulations focused on the CBS area. The adopted procedure was analogous to the one introduced for the system with the DES spacer[35] and is here briefly summarized. The protein surface was docked considering the ligand already bound to the spacer, to account for the steric hindrance of the AG chains that are to be bound to the spacer when the initial structure of the MD simulations is set up. However, a different flexibility was defined for two molecules: the sp^3 bonds of A2P were left free to rotate, while none of the bonds of the spacer were rotatable. The search box was centered on the CBS and large enough to allow the spacer−A2P pair to rotate freely; it consisted of a grid of $60 \times 60 \times 60$ points with a spacing of 0.375 Å. Docking was carried out holding the Fc domain fixed and letting the ligand move over its surface; for each spacer−A2P pair about 50 poses were evaluated using a Lamarckian genetic algorithm.[44] The optimal pose is characterized by having the A2P−spacer pair located in the consensus binding site, the spacer turned toward the solvent, facing thereby the binding AG, and provided hence the minimum energy. Docking energies of the best 15 poses for each spacer−A2P pair are summarized in the Supporting Information. For the DES, SS3, and TRZ spacers, the first pose was chosen for the MD simulations, as it satisfied all of the requirements described above. For the 2LP spacer, instead, the 12th pose was considered since in the ones with higher interaction energy the spacer tended to align along the protein surface. The selected poses are very similar and indicate that the formation of the complex between A2P and IgG involves some specific residues of the antibody, which can be subdivided in three groups: HIS-310, GLN-311, and LEU 314 is the first, MET-428, ASN-434, and HIS-435 the second, and ILE-253 and SER-254 the third (Figure 6a). It can be noted that these are the same residues involved in the interaction of IgG with several natural and synthetic ligands.[25]

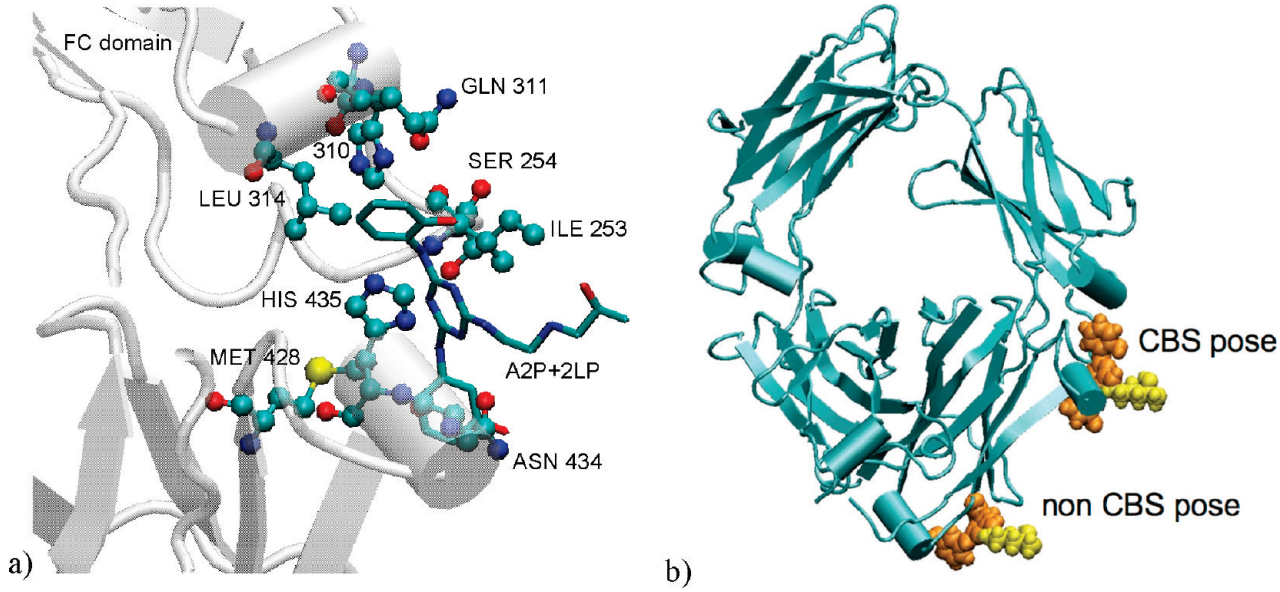

Figure 6. (a) Detail of the docking pose of the 2LP−A2P pair in the CBS; (b) comparison between the CBS and the non CBS pose.

This evidence is not surprising as A2P was specifically designed to mimic the interactions of the PHE 132−TYR 133 pair of protein A with IgG. It seems likely that also the spacer contributes to the interaction, as shown by the different docking energies of the A2P−spacer pairs.

To fully understand the properties of the consensus binding site, a system in which the initial pose of the ligand is not in the CBS was considered. For this investigation the 2LP spacer was chosen and also in this case the initial structure of the system was determined through docking. No significant differences in the docking energies of the CBS and non CBS complexes can be noted. In the chosen non CBS pose, sketched in Figure 6a, A2P is interacting with residues from SER-384 to GLU-389 and from ARG-417 to TRP-424 of one of the CH3 chains of the Fc domain.

Analysis of the Interaction between IgG and A2P Supported on AG. The conformational evolution of the complex consisting of full Fc domain, A2P, spacer, and AG was studied using 15 ns MD simulations. The A2P-DES complex was described in a previous publication, in which the effect of the interaction between ligand and support on the binding process was discussed.[35] In the present work, three new spacers (2LP, TRZ, and SS3) were introduced to investigate their influence on the conformational and energetic evolution of the complex.

The conformational analysis of the MD simulations shows that, as found for DES,[35] also when other spacers are used A2P has a certain mobility within the binding site. However in the investigated time span the ligand never leaves the CBS, thus confirming the stability of this binding structure. The simulated complexes exhibit a similar dynamic behavior in the investigated time span. The first nanoseconds of the simulation are characterized by the approach of the Fc domain to the support and the establishment of some interactions between the two macromolecules. The partial adsorption of the antibody on AG leads to a small reorganization of its structure, which is accompanied by a distortion of the spacer that abandons its initial elongated structure and partially folds on itself, probably to favor the establishment of an energetically preferred orientation between protein and AG. This is observed even in the case of 2LP, which is the shortest among the considered spacers. The initial and final structures assumed by the complexes are reported as Supporting Information.

The evolution of van der Waals and electrostatic interactions throughout the MD simulations is reported for all spacers in Figure 7. It can be noted that each system generally reaches an energetically stable configuration within the first 5 ns of simulation, after which only minor fluctuations are observed. An exception to this trend is given by A2P-2LP. In fact, though its average interaction energy, defined as sum of electrostatic and van der Waals terms, is constant between 5 and 12 ns, it oscillates significantly toward the end of the simulation. The analysis of the system structural evolution revealed that the energy oscillation can be attributed to a transient reorganization of A2P-2LP in the binding site, which leads to a temporary loss of electrostatic interactions of the spacer with the surrounding environment. Such oscillation, of statistical nature and determined by the high A2P-2LP mobility, leads to a slight decrease of the A2P interaction energy with IgG. It is not unlikely that the continuation of the simulations for a longer time span would smooth down this energy oscillation. The energy plots reported in Figure 7 give a first indication on the relative performances of the spacers, according to which TRZ has the highest interaction energy, followed by 2LP, DES, and SS3, which interaction energy is slightly positive.

To investigate in greater detail the influence of the spacer on the interaction of the ligand with both the support and the antibody, average interaction energies of the spacer-A2P pair with the surrounding environment in the free (i.e., when only the water surrounds the AG−spacer−A2P system) and bound state (i.e., when the ligand is in a complex with the antibody) were calculated and are reported in Table 2. For all systems the establishment of binding interactions between ligand and antibody is determined mostly by van der Waals forces, as expected for molecules designed to have a high affinity for a hydrophobic receptor. It is interesting to notice that the systems in which $\Delta V^{vdw}_{free\rightarrow bound}$ is the lowest (about −20 kcal/mol) are those with the TRZ and SS3 spacers; however, the van der Waals interaction energy is mostly counterbalanced by the loss of electrostatic interactions. As previously observed for the system with the DES spacer,[35] it can be noted that for all spacers except TRZ, the formation of significant interactions between the ligand and the AG support leads to the most pronounced hindrance in the interaction of A2P with the antibody. The system with the TRZ spacer is the only one in which, in the

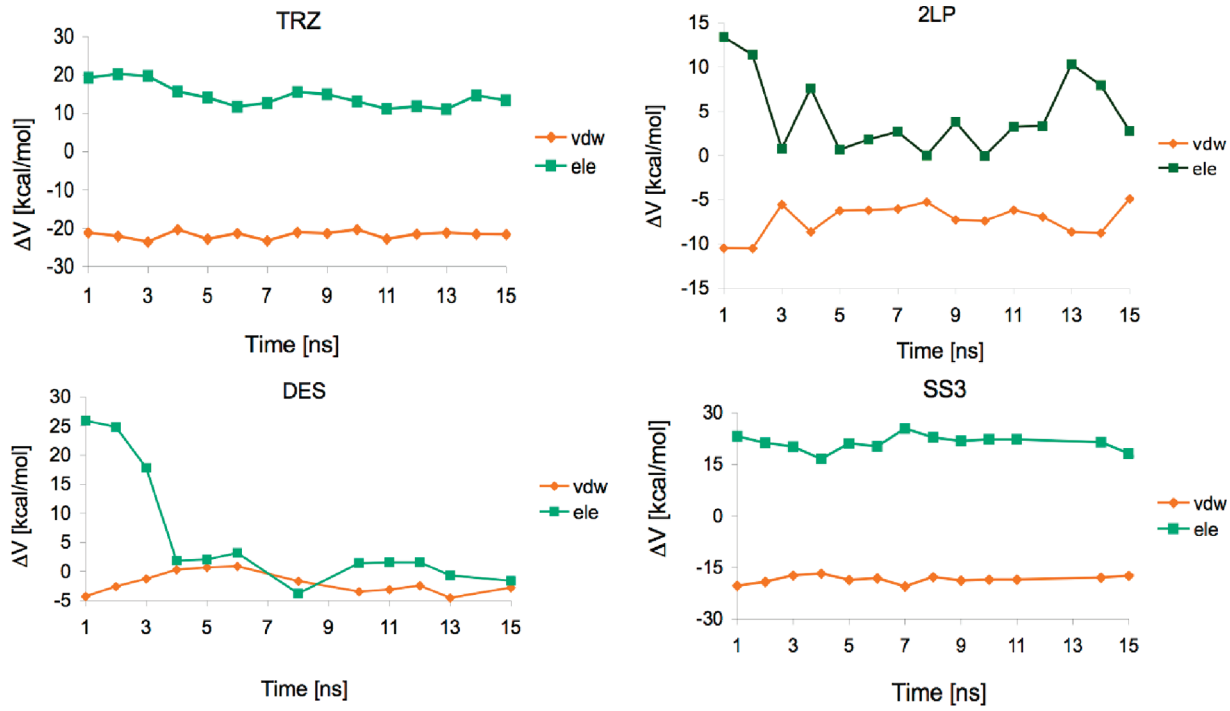

Figure 7. Electrostatic (ele) and van der Waals (vdw) interaction energies between immobilized A2P ligand and IgG evaluated as a function of simulations time and averaged on time spans of 1 ns.

TABLE 2: Electrostatic (ele) and van der Waals (vdw) Average Interaction Energies Evaluated in the 5−15 ns Time Span for the Spacer−A2P Pair Supported on AG with the Initial Pose in the CBS

		2LP	DES	TRZ	SS3
Free System (Support−Spacer−A2P)					
H_2O[a]	vdw	−23.94	−27.76	−29.90	−28.20
	ele	−78.66	−87.96	−87.93	−75.74
support	vdw	−17.67	−29.93	−7.12	−12.07
	ele	−16.71	−16.51	1.98	−8.01
Bound System (Support−Spacer−A2P−FC)					
H_2O + FC	vdw	−46.29	−55.79	−50.44	−56.77
	ele	−85.82	−102.12	−72.21	−63.43
support	vdw	−2.06	−3.93	−8.47	−1.99
	ele	−6.30	−1.88	0.58	1.38
ΔV (Bound − Free)					
H_2O + FC	vdw	−22.35	−28.03	−20.54	−28.57
	ele	−7.16	−14.15	15.72	12.32
support	vdw	15.61	26.00	−1.35	10.07
	ele	10.42	14.63	−1.40	9.39
Total ΔV					
H_2O + FC + support	vdw	−6.70	−2.03	−21.89	−18.50
	ele	3.32	0.48	14.32	21.71

[a] The first column reports the contribution of the surrounding environment (H_2O, Fc, and support) considered to evaluate the interaction of the spacer-A2P pair.

free state, the ligand does not strongly interact with AG. The simulations have in fact evidenced that it continuously shifts from the solvated to the adsorbed conformation. On the contrary, when the 2LP, SS3 and DES spacers were adopted it was found that A2P, when IgG is not present, is predominantly adsorbed on the support. This analysis leads to the conclusion that, from an energetic standpoint, the best performing spacers are either those with a relatively high length and flexibility (DES, TRZ) or those that possess some electrostatic groups that can contribute to increase the electrostatic interaction energy with the protein (2LP, TRZ). TRZ, the spacer that emerged from the experiments as that with the best performances, is the only one that satisfies both requirements.

In order to test whether the size of the AG molecular model could affect the results of the simulations, additional calculations were performed adopting an enlarged AG molecular model developed following the procedure described in the method section. The molecular structure reached by the system after 10 ns of simulations is sketched in Figure 8. The structure so determined is qualitatively similar to that calculated employing the smaller AG molecular model, reported in Figure S2, thus giving a first confirmation of the reliability of the adopted computational procedure. A second, and more important confirmation comes from the calculation of the interaction energies between A2P and IgG, reported as Figure S5, which shows that the energy determined for the model implementing the large molecular surface is similar to the one calculated adopting the smaller, and computationally more tractable, AG molecular model.

Analysis of the Interaction between IgG and A2P for a Non-CBS Binding Site. The molecular systems described in the previous paragraph was adopted as initial structure for the MD simulation of a docking pose in which the A2P molecule is interacting with the main binding site of the Fc domain of IgG: the CBS. However other binding sites, different from the CBS, were identified in the docking analysis. The purpose of this section is therefore to study the interactions developed between IgG and A2P for a binding site different from the CBS. The ligand-spacer system chosen to perform this analysis is A2P-2LP, i.e. the experimental benchmark. The starting structure for the simulations was determined by docking and involves an interaction site located on one of the CH3 chains of the Fc domain of IgG.

The final conformation reached by the system after 15 ns of simulation is shown in Figure 9. From a macroscopic viewpoint, the structure of Figure 9 is similar to that reached in the simulations performed for the CBS binding site, in which the antibody partially interacts with AG through one of its CH

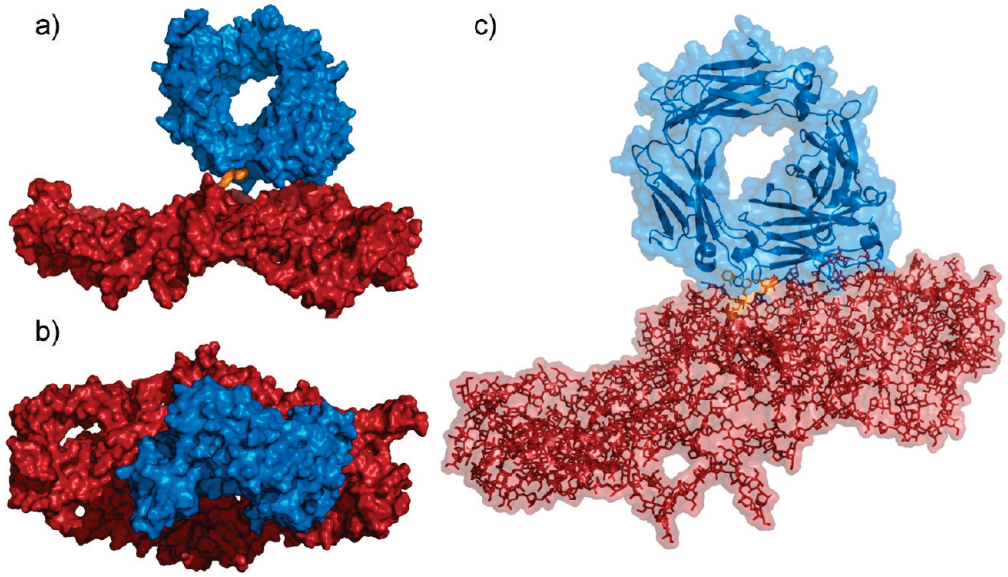

Figure 8. Structure reached by the A2P-2LP-AG model after 10 ns of simulation: (a) front, (b) top, and (c) three-quarter views.

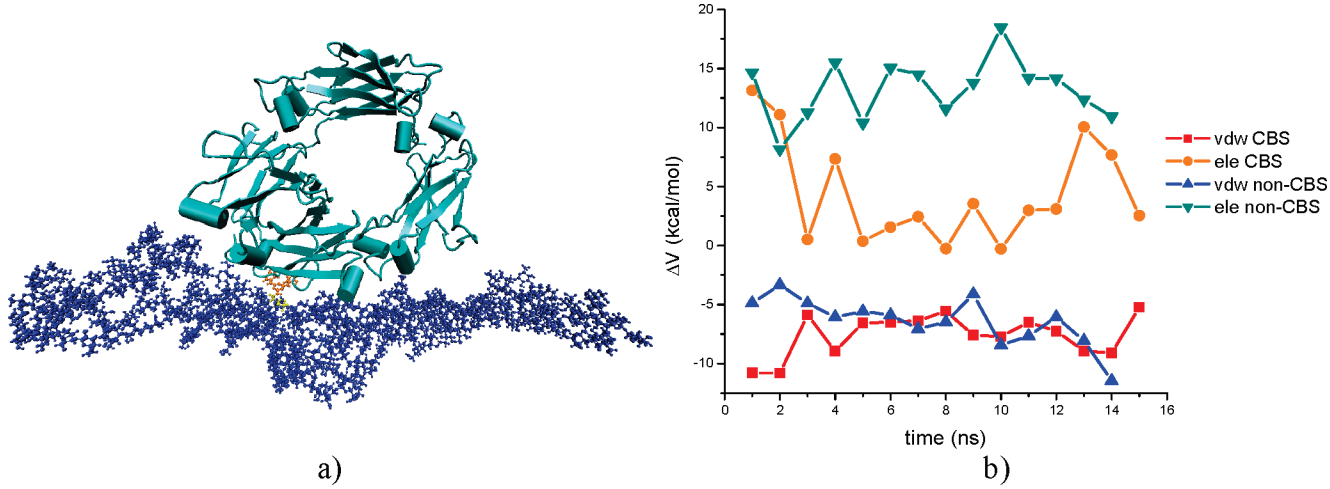

Figure 9. A2P−2LP pair in the non CBS pose: (a) structure after 15 ns of simulation and (b) van der Waals (vdw) and electrostatic (ele) interaction energies of A2P and 2LP with the surrounding environment between free and bound state for CBS and non CBS systems.

TABLE 3: Electrostatic (ele) and van der Waals (vdw) Interaction Energies of A2P and 2LP with the Fc Domain and the Solvent Evaluated after 10 ns of MD Simulation: Comparison between CBS and Non CBS Complexes

	FC				H_2O			
	2LP		A2P		2LP		A2P	
	vdw	ele	vdw	ele	vdw	ele	vdw	ele
free system					−4.94	−25.92	−19.00	−52.92
CBS pose	−2.79	−0.21	−31.22	−9.63	−5.23	−33.62	−7.31	−44.13
non CBS pose	−4.67	−9.69	−22.09	−11.94	−4.96	−26.37	−13.06	−31.51
Δ (CBS-non CBS)	1.88	9.48	−9.13	2.31	−0.27	−7.25	5.75	−12.62

domains. However, the energetic analysis of the MD simulations indicates significant differences in the interactions established by the A2P−2LP pair with IgG, when located in these two binding sites. Since the energetics of the system in the absence of the Fc domain is the same as for the CBS system, the comparison can be based on the interactions developed in the bound system, which is shown in Figure 9b. It can thus be observed that while the van der Waals interaction energy established by the A2P−2LP pair with the surrounding environment (support, solvent and antibody) is similar for both binding sites, electrostatic interactions are significantly less favorable for the non CBS structure. This is mainly due to the loss of interactions of the A2P−2LP pair with the solvent+antibody environment (about 7.2 kcal/mol) rather than with the support (about 3.3 kcal/mol).

A detailed analysis was performed on the 10th nanosecond of both simulations to break down the interaction energy contribution given by the Fc domain from that of water (Table 3). It is interesting to note that the van der Waals interactions present significant differences in the two cases, which however cancel out when considered together. In particular, van der Waals interactions of A2P with the Fc domain are prevailing in the CBS complex, as expected, but are counterbalanced by the weaker electrostatic interactions established by 2LP. It is also interesting to observe the effect that the solvent has on the stability of the complex: in the CBS pose the electrostatic

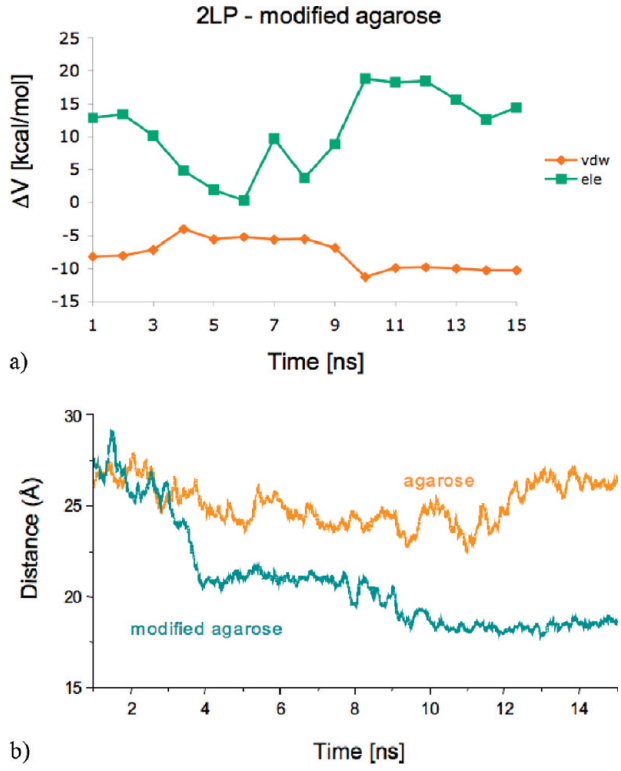

Figure 10. (a) Energies of the complex supported on AG modified with 6-*O*-methyl-galactose residues. (b) Distance between a support key residue and the center of mass of one of the CH3 chains of the Fc domain: AG (green) and AG modified with 6-*O*-methyl-galactose units (orange).

interactions with both ligand and spacer are considerably stronger than in the non CBS pose, which can be mostly ascribed to the fact that in the CBS complex the accessibility to water is significantly larger than in the non CBS pose, in which ligand and spacer are sandwiched between protein and support, which leads thus to a partial desolvation of this area.

Analysis of the Interaction between IgG and A2P Supported on Modified AG. To fully understand the performances of a chromatographic system, it is necessary to investigate the influence of the chemical nature of the support material on the binding process. Thus the AG surface was modified by substituting part of the galactose residues with 6-*O*-methyl-galactose units in order to obtain a more hydrophobic support, as previously described in the Methods section. The chosen spacer was also in this case 2LP and the initial structure of the complex was identical to the one adopted for A2P-2LP. The analysis of the evolution of the free binding energy with the simulation time is shown in Figure 10a. In the first 9 ns of simulation the energy of the complex seems to stabilize and to follow a trend similar to that observed for the AG support, though the average interaction energy in this first time span is slightly higher (see Figure 7). However, in the following 5 ns, the complex undergoes a conformational change, as the Fc domain further approaches the support. The average value of the interaction energy in this final time span is positive by about 6 kcal/mol, thus significantly larger than that calculated for the AG surface (about −3 kcal/mol, see Table 3).

In order to quantify the extent of this interaction, the mean distance between one of the residues of the support that plays a key role in the interaction with the antibody and the center of mass of one of the CH3 chains of the Fc domain was calculated and plotted in Figure 10b. As it can be observed, while the initial mean distance is similar for both simulations (about 27 Å) in the first 3 ns, which is determined by the similar molecular conformation from which the simulations are started, the situation changes significantly as the system evolves. In fact, while in the case of AG this distance stabilizes at a mean value of about 25 Å, in the case of the modified support it decreases in two steps first to about 21 Å (3−9 ns) and then to 18.4 Å in the last 5 ns.

The energetic and structural evidence can be rationalized in terms of the establishment of interactions between ligand and hydrophobic surface that are competitive with those formed by the affinity ligand in the CBS, which final result is the destruction of the interaction between support and affinity ligand. Though this is clearly a limiting case, this result however indicates that the molecular properties of the surface surrounding the affinity ligand can influence greatly the binding process, up to the point of leading to the loss of affinity, and thus selectivity, of the material.

Analysis of the Interaction between Pluronic F68 and A2P Spacers. The experimental data reported and discussed in the experimental section clearly showed that the presence of Pluronic acid in solution affects considerably the performances of the A2P-2LP couple, decreasing its capability to interact with IgG, while its effect is almost negligible for other spacers, such as SS3 or TRZ. To investigate this aspect in detail, some additional simulations focused on the individuation of interactions between Pluronic F68 and the 2LP, SS3, and TRZ spacers were performed. Considering the difficulty of building a reliable molecular model of Pluronic F68 and the relatively small size of the chosen spacers, it was decided to model the interaction between the two molecules using representative molecular fragments for each of them. In particular, it was decided to model Pluronic F68 as ethylene dimethyl ether (EDME), the spacers using the full structure sketched in Figure 1, and A2P only through its triazine core. The rationale for the development of these models lies in the particular nature of the 2LP spacer, where the amino group positioned furthest from the A2P ligand is protonated, and thus charged, in the conditions at which the IgG adsorption process is usually performed. This suggests that a possible explanation for the different behavior of A2P-2LP with respect to other ligand-spacer couples might be the establishment of interactions involving the charged amino group. Following this lead, minimum energy structures of the complexes formed by A2P-2LP/SS3/TRZ and EDME were searched by systematic docking followed by energy minimization protocols performed at the B3LYP/6-31 g(d,p) level considering implicitly the solvent using the IEFPCM model. The calculated minimum energy interaction structures, which XYZ coordinated are reported in the Supporting Information, are reported in Figure 11.

The structures reported in Figure 11 evidence that a hydrogen bond involving directly the spacer arm is formed only for the A2P-2LP - EDME complex and involves directly the ether atom of EDME and the amino group. The interaction energies of the three complexes, computed at the B3LYP/aug-cc-pVTZ level, are −0.87, 0.0, and −0.35 kcal/mol for the complexes involving A2P-2LP, A2P-TRZ, and A2P-SS3, respectively. This supports the initial hypothesis that Pluronic F68 is able to establish significant interactions with the 2LP spacer, which might be responsible for the enhanced sensitivity to Pluronic F68 observed for 2LP materials.

Comparison between Experiment and Theory. After having obtained sufficient experimental and theoretical results of ligand, spacer and support interactions as well as information

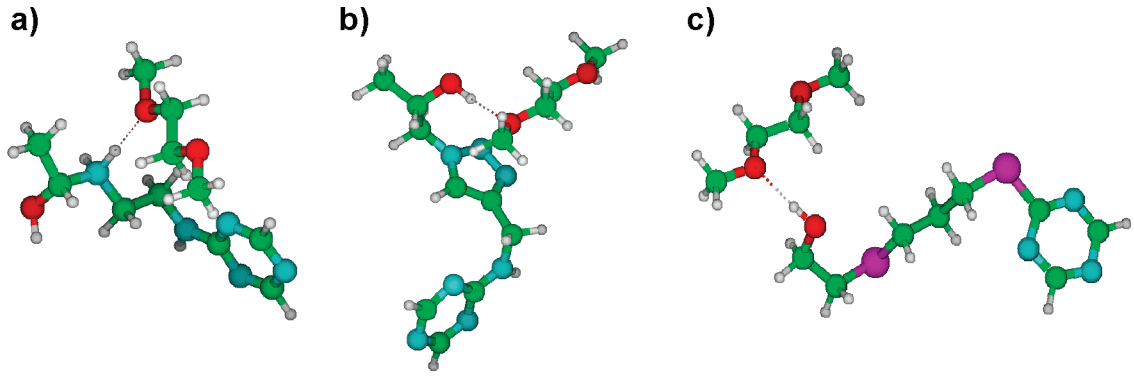

Figure 11. Minimum energy structures of the complexes between ethylene dimethyl ether and (a) A2P-2LP, (b) A2P-TRZ, and (c) A2P-SS3.

about the interaction between the ligand-spacer combination and the antifoaming additive Pluronic F68, the computational results can be adopted to interpret the experimental evidence.

Effect of Spacer Chemistry. Simulations performed for the reference AG support for the different spacers considered can be directly compared to experimental data measured for the F3 feed (pure IgG) when the support is AG (Figure 3b). It is interesting to observe that, while the calculated interaction energies depend substantially from the adopted spacer, with TRZ based materials predicted to be those with the highest energy of interaction, experimentally no significant differences can be observed. Two concurring effects are most likely responsible for such behavior. The first is that the material has probably reached saturation, which is supported by the fact that the measured DBC for A2P materials are similar to those determined using protein A affinity chromatography. The second is that the differences among the free interaction energies (ΔG) between material and support, that determine the binding constants, are reduced with respect to those calculated among the interaction energies (ΔH) by an entropy−enthalpy compensation effect. This is directly confirmed by free interaction energies calculated adopting the linear interaction energy (LIE) protocol,[52] following the procedure outlined in our previous publications[24,35] and using the van der Waals and electrostatic interaction energies reported in Table 3, scaled using standard LIE parameters.[53] LIE interaction energies calculated for the four spacers differ in fact by no more than 1 kcal/mol for the TRZ, 2LP, and DES spacer, while calculations predict that materials exploiting the SS3 spacer should perform worse than the others. Interestingly, this is confirmed by experiments (Figure 3).

For the F2 feed, TRZ on AG performs better than SS3 and 2LP. With the F1 feed on Fractogel, in the presence of Pluronic F68, TRZ performs significantly better than SS3 and DES. From a theoretical standpoint, the high performances of the TRZ spacer, which DBC is comparable to that of Rmp protein A Sepharose FF, can be related to the finding that this is the only spacer which, when not bound to IgG, has no significant interaction with the support. Also, this is the spacer for which we computed the highest interaction energy with IgG. This can indeed be considered as one of the main findings of this investigation, which supports the hypothesis advanced in our previous study[24] that the interaction of the ligand with the support can have a major impact on the performances of the separation process. In addition, the present work indicates that the best separation performances are obtained when the spacer-ligand pair is not interacting with the surface and is thus highly mobile. This is the motivation for the high interaction energies calculated for the A2P−TRZ system, which, though probably reduced by a significant entropy compensation effect (an indirect measure of the mobility of the ligand-spacer pair, that is directly related to conformational entropy), is responsible for the high performances obtained when using this specific spacer.

Effect of Support Chemistry. Both experiments and theory confirm that not only the ligand headgroup, A2P, but also the spacer and the support chemistry contribute significantly to the capture of IgG. Simulations predict that a more hydrophobic surface reduces the affinity of the ligand for the antibody. This might explain the decrease of IgG capture capability observed experimentally, which is highest for the AG-based matrixes, decreases for Fractoprep and reaches a minimum for Fractogel. In particular, the binding capacity for IgG increases by a factor of 3 (for F1) when changing the support from Fractogel to Fractoprep. This is reasonable as it can be expected that AG is more hydrophilic than Fractoprep, which is a hydrophilic synthetic polyvinylether cross-linked with acrylamide molecules, and Fractogel, a polymethacrylate based support.

Calculations show that a modification of the support structure, consisting in the insertion of OCH_3 groups, leads to a significant decrease of the energy of interaction between ligand and protein. The origin of this effect is 2-fold, since a change of support shows an impact on both the energy of interaction of the ligand with the support, which must be overcome to let the ligand bind the protein, and on the direct interaction between protein and support.

Effect of Surface Chemistry. It is obvious that besides the bare support chemistry, any modification of the support surface can induce a change of the overall properties of an adsorbent. While the thioether based spacers as well as the mercaptoethanol end-capping are noncharged, but rather hydrophobic in nature, the incorporated amino functionality of 2LP and the ethanolamine end-capping exhibit weak anion exchange properties. An extreme case is the introduction of azido groups, which are rather hydrophilic in nature and bind IgG due to electron donor/acceptor interactions as well as due to the fact that IgG possesses hydrophobic patches on its surface. This additional interaction between surface-bound azide and IgG molecules leads most probably to an increased IgG binding performance of the TRZ-type adsorbents.

Effect of Ligand Density. Since this study evidenced the importance of the surface structure, it is important to point out that the density of A2P ligands on the surface influences the IgG capture rate by establishing multiple interactions or, more simply, by modifying the surface properties. Theoretical calculations support the latter interpretation, since docking and successive MD simulations clearly indicated that the dominating binding site of IgG is the CBS. Moreover, the simulations clearly show that a modification of the surface properties can have a significant impact on the materials performances, since, as shown above and confirmed by experiments, a surface that is

able to establish significant van der Waals interaction with the protein may even disrupt the CBS interaction.

Effect of Pluronic F68 in the Feed. Experiments with the F1 feed show that materials with the 2LP spacer perform in general better than those with the other spacers. However, when Pluronic acid is added, the introduction of the SS3 or TRZ spacer arm results in an increased binding of IgG compared to adsorbents with 2LP spacers. A similar trend is seen with F2 where the SS3 and TRZ containing adsorbents bind more IgG than AG-2LP-A2P. In particular in the case of AG-TRZ-A2P the binding capacity is even comparable to that achieved for the bench mark adsorbent Rmp protein A Sepharose FF. This is different than what was observed for the pure feed F3, and confirmed by calculations, according to which 2LP should perform similarly to DES and TRZ. The main reason for the deviation of experimental results for the three different spacers is the fact that the composition of the test solutes is very different in their complexity. The main difference between F1 and F3 is the presence of other proteins in the feed and Pluronic acid. It can therefore be reasonably concluded that the different performances can be attributed to competitive interactions of the affinity matrix with other macromolecules present in solution besides the target protein IgG. On the basis of the experimental and theoretical calculations performed to investigate this aspect, two interpretations are possible. The first is that, if Pluronic acid is interacting with the AG surface, then the presence of the TRZ and SS3 spacer arms appear to push the ligand far enough away from the AG surface to enable the ligand to capture IgG. The second is that it is the spacer itself that contributes to increase the interaction energy between Pluronic acid and the support surface functionalized with A2P ligands. The latter interpretation is supported by computational evidence, indicating that the charged amino group of the 2LP spacer can establish some binding electrostatic interaction with the etheric oxygen atoms of Pluronic acid. The competitive adsorption of Pluronic acid on a surface functionalized with 2LP-A2P provides a reasonable explanation of the reason why the 2LP-A2P pair observes a reduction of binding capacity for IgG, when Pluronic acid is present in solution.

4. Summary and Conclusions

As a final remark, it can be concluded that a combined approach exploiting experiments and MD simulations appears as a useful tool for the design of new materials. The simulation results indicate that it is important, when screening ligand libraries, to account for the interaction of the ligand with the support. This is valid both, when designing a new ligand in silico as well as when searching experimentally with a combinatorial library approach, since a viable ligand candidate that was originally tested on one support might behave quite differently on another (more hydrophilic/hydrophobic) and might at the end even perform much better than with the former. The influence of ligand−support interaction on the protein binding process can in actual fact be quite significant, especially if it is competitive to the ligand-protein interaction.

Since the accuracy of the prediction of MD simulations is also satisfactory with more complex sample matrices it can be overall stated that with increasing knowledge of the interaction properties of the participating moieties of ligand, spacer, support and target analyte during the capture of the latter, the more reliable the corresponding predictions obtained by computer simulation studies will be. MD simulations are surely an excellent tool, both, for the prediction of binding capacities in simple feed matrices as well as for the interpretation of experimental results.

Acknowledgment. The authors acknowledge the European Commission (EU) for funding this research work, performed under the integrated project AIMs (Advanced Interactive Materials by Design; Contract No. NMP3-CT2004-500160), which was part of the 6th Framework Program of the EU. ProMetic BioSciences is a trademark of ProMetic BioSciences Ltd; PuraBead is registered with the U.S. Patent & Trademark Office; MAbsorbent is registered with the U.S. Patent & Trademark Office; Chemical Combinatorial Library is registered with the U.K. Patent & Trademark Office.

Supporting Information Available: The protocols for the preparation of all here-investigated ligands and materials as well as their experimental evaluation. This material is available free of charge via the Internet at http://pubs.acs.org.

References and Notes

(1) Waldmann, T. A.; Levy, R.; Coller, B. S. *Hematology* **2000**, *2000*, 394.
(2) Saphire, E. O.; Parren, P.; Pantophlet, R.; Zwick, M. B.; Morris, G. M.; Rudd, P. M.; Dwek, R. A.; Stanfield, R. L.; Burton, D. R.; Wilson, I. A. *Science* **2001**, *293*, 1155.
(3) Scallon, B. J.; Snyder, L. A.; Anderson, G. M.; Chen, Q. M.; Yan, L.; Weiner, L. M.; Nakada, M. T. *J. Immunother.* **2006**, *29*, 351.
(4) MacConnachie, A. M. *Intensive Crit. Care Nurs.* **2000**, *16*, 123.
(5) Keller, K.; Friedmann, T.; Boxman, A. *Trends Biotechnol.* **2001**, *19*, 438.
(6) Roque, A. C. A.; Lowe, C. R.; Taipa, M. A. *Biotechnol. Prog.* **2004**, *20*, 639.
(7) Lowe, C. R. *Curr. Opin. Chem. Biol.* **2001**, *5*, 248.
(8) Labrou, N. E. *J. Chromatogr. B* **2003**, *790*, 67.
(9) Clonis, Y. D. *J. Chromatogr. A* **2006**, *1101*, 1.
(10) Hahn, R.; Shimahara, K.; Steindl, F.; Jungbauer, A. *J. Chromatogr. A* **2006**, *1102*, 224.
(11) Hahn, R.; Bauerhansl, P.; Shimahara, K.; Wizniewski, C.; Tscheliessnig, A.; Jungbauer, A. *J. Chromatogr. A* **2005**, *1093*, 98.
(12) Roque, A. C. A.; Silva, C. S. O.; Taipa, M. A. *J. Chromatogr. A* **2007**, *1160*, 44.
(13) Hober, S.; Nord, K.; Linhult, M. *J. Chromatogr. B* **2007**, *848*, 40.
(14) Fassina, G.; Ruvo, M.; Palombo, G.; Verdoliva, A.; Marino, M. *J. Biochem. Biophys. Methods* **2001**, *49*, 481.
(15) Fassina, G.; Verdoliva, A.; Odierna, M. R.; Ruvo, M.; Cassini, G. *J. Mol. Recognit.* **1996**, *9*, 564.
(16) Braisted, A. C.; Wells, J. A. *Proc. Natl. Acad. Sci. U.S.A* **1996**, *93*, 5688.
(17) Dias, R. L. A.; Fasan, R.; Moehle, K.; Renard, A.; Obrecht, D.; Robinson, J. A. *J. Am. Chem. Soc.* **2006**, *128*, 2726.
(18) Yang, H. G. P. V.; Carbonell, R. G. *J. Pept. Res.* **2005**, *66*, 120.
(19) Li, R. X.; Dowd, V.; Stewart, D. J.; Burton, S. J.; Lowe, C. R. *Nat. Biotechnol.* **1998**, *16*, 190.
(20) Teng, S. F.; Sproule, K.; Hussain, A.; Lowe, C. R. *J. Mol. Recognit.* **1999**, *12*, 67.
(21) Teng, S. F.; Sproule, K.; Husain, A.; Lowe, C. R. *J. Chromatogr. B* **2000**, *740*, 1.
(22) Newcombe, A. R.; Cresswell, C.; Davies, S.; Watson, K.; Harris, G.; O'Donovan, K.; Francis, R. *J. Chromatogr. B* **2005**, *814*, 209.
(23) Feng, H. L. J.; Li, H.; Wang, X. *Biomed. Chromatogr.* **2006**, *20*, 1109.
(24) Busini, V.; Moiani, D.; Moscatelli, D.; Zamolo, L.; Cavallotti, C. *J. Phys. Chem. B* **2006**, *110*, 23564.
(25) DeLano, W. L.; Ultsch, M. H.; de Vos, A. M.; Wells, J. A. *Science* **2000**, *287*, 1279.
(26) Mateo, C.; Abian, O.; Ernedo, M. B.; Cuenca, E.; Fuentes, M.; Fernandez-Lorente, G.; Palomo, J. M.; Grazu, V.; Pessela, B. C. C.; Giacomini, C.; Irazoqui, G.; Villarino, A.; Ovsejevi, K.; Batista-Viera, F.; Fernandez-Lafuente, R.; Guisan, J. M. *Enzyme Microb. Technol.* **2005**, *37*, 456.
(27) Guisan, J. M. *Enzyme Microb. Technol.* **1988**, *10*, 375.
(28) Fernandez-Lafuente, R.; Rosell, C. M.; Rodriguez, V.; Santana, C.; Soler, G.; Bastida, A.; Guisán, J. M. *Enzyme Microb. Technol.* **1993**, *15*, 546.
(29) Fuentes, M.; Mateo, C.; Fernandez-Lafuente, R.; Guisan, J. M. *Biomacromolecules* **2006**, *7*, 540.
(30) Moses, J. E.; Moorhouse, A. D. *Chem. Soc. Rev.* **2007**, *36*, 1249.
(31) Binder, W. H.; Sachsenhofer, R. *Macromol. Rapid Commun.* **2007**, *28*, 15.
(32) Tornoe, C. W.; Christensen, C.; Meldal, M. *J. Org. Chem.* **2002**, *67*, 3057.

(33) Cuatrecasas, P.; Wilchek, M.; Anfinsen, C. B. *Proc. Natl. Acad. Sci. U.S.A.* **1968**, *61*, 636.
(34) Wilchek, M.; Miron, T. *React. Funct. Polym.* **1999**, *41*, 263.
(35) Zamolo, L.; Busini, V.; Moiani, D.; Moscatelli, D.; Cavallotti, C. *Biotechnol. Prog.* **2008**, *24*, 527.
(36) Arnott, S.; Fulmer, A.; Scott, W. E.; Dea, I. C. M.; Moorhouse, R.; Rees, D. A. *J. Mol. Biol.* **1974**, *90*, 269.
(37) Kirschner, K. N.; Woods, R. J. *Proc. Natl. Acad. Sci. U.S.A.* **2001**, *98*, 10541.
(38) Kirschner, K. N.; Woods, R. J. *J. Phys. Chem. A* **2001**, *105*, 4150.
(39) Basma, M.; Sundara, S.; Calgan, D.; Vernali, T.; Woods, R. J. *J. Comput. Chem.* **2001**, *22*, 1125.
(40) Kirschner, K. N.; Tschampel, S.; Woods, R. GLYCAM04 force field, 2004.
(41) Cornell, W. D.; Cieplak, P.; Bayly, C. I.; Gould, I. R.; Merz, Jr., K. M.; Ferguson, D. M.; Spellmeyer, D. C.; Fox, T.; Caldwell, J. W.; Kollman, P. A. *J. Am. Chem. Soc.* **1995**, *117*, 5179.
(42) Case, D. A.; Darden, T. A.; Cheatham, III, T. E.; Simmerling, C. L.; Wang, J.; Duke, R. E.; Luo, R.; Merz, K. M.; Wang, B.; Pearlman, D. A.; Crowley, M.; Brozell, S.; Tsui, H.; Gohlke, H.; Mongan, J.; Hornak, V.; Cui, G.; Beroza, P.; Schafmeister, C.; Caldwell, J. W.; Ross, W. S.; Kollman, P. A. *AMBER 8*; University of California: San Francisco, 2004.
(43) Case, D. A.; Cheatham, T. E.; Darden, T.; Gohlke, H.; Luo, R.; Merz, K. M.; Onufriev, A.; Simmerling, C.; Wang, B.; Woods, R. J. *J. Comput. Chem.* **2005**, *26*, 1668.
(44) Morris, G. M.; Goodsell, D. S.; Halliday, R. S.; Huey, R.; Hart, W. E.; Belew, R. K.; Olson, A. J. *J. Comput. Chem.* **1998**, *19*, 1639.
(45) Frisch, M. J.; Trucks, G. W.; Schlegel, H. B.; Scuseria, G. E.; Robb, M. A.; Cheeseman, J. R.; Montgomery, J. A., Jr.; Vreven, T.; Kudin, K. N.; Burant, J. C.; Millam, J. M.; Iyengar, S. S.; Tomasi, J.; Barone, V.; Mennucci, B.; Cossi, M.; Scalmani, G.; Rega, N.; Petersson, G. A.; Nakatsuji, H.; Hada, M.; Ehara, M.; Toyota, K.; Fukuda, R.; Hasegawa, J.; Ishida, M.; Nakajima, T.; Honda, Y.; Kitao, O.; Nakai, H.; Klene, M.; Li, X.; Knox, J. E.; Hratchian, H. P.; Cross, J. B.; Bakken, V.; Adamo, C.; Jaramillo, J.; Gomperts, R.; Stratmann, R. E.; Yazyev, O.; Austin, A. J.; Cammi, R.; Pomelli, C.; Ochterski, J. W.; Ayala, P. Y.; Morokuma, K.; Voth, G. A.; Salvador, P.; Dannenberg, J. J.; Zakrzewski, V. G.; Dapprich, S.; Daniels, A. D.; Strain, M. C.; Farkas, O.; Malick, D. K.; Rabuck, A. D.; Raghavachari, K.; Foresman, J. B.; Ortiz, J. V.; Cui, Q.; Baboul, A. G.; Clifford, S.; Cioslowski, J.; Stefanov, B. B.; Liu, G.; Liashenko, A.; Piskorz, P.; Komaromi, I.; Martin, R. L.; Fox, D. J.; Keith, T.; Al-Laham, M. A.; Peng, C. Y.; Nanayakkara, A.; Challacombe, M.; Gill, P. M. W.; Johnson, B.; Chen, W.; Wong, M. W.; Gonzalez, C.; Pople, J. A. Gaussian 03, revision C.01; Gaussian, Inc.: Wallingford, CT, 2004.
(46) Schaftenaar, G.; Noordik, J. H. *J. Comput.-Aided Mol. Des.* **2000**, *14*, 123.
(47) Humphrey, W.; Dalke, A.; Schulten, K. *J. Mol. Graph.* **1996**, *14*, 33.
(48) DeLano, W. L. The PyMOL Molecula Graphics System, on world wide web http://www.pymol.org2002.
(49) Chhatre, S.; Titchener-Hooker, N. J.; Newcombe, A. R.; Keshavarz-Moore, E. *Nat. Protoc.* **2007**, *2*, 1763.
(50) Yang, H.; Gurgel, P. V.; Carbonell, R. G. *J. Chromatogr., A* **2009**, *1216*, 910.
(51) Horak, J.; Hofer, S.; Lindner, W. *J. Chromatogr. B*, **2010**, to be submitted.
(52) Carlsson, J.; Ander, M.; Nervall, M.; Aqvist, J. *J. Phys. Chem. B* **2006**, *110*, 12034.
(53) Aqvist, J.; Hansson, T. *J. Phys. Chem.* **1996**, *100*, 9512.

JP1017168